PHYSICAL REVIEW B 107, 024512 (2023)

Editors' Suggestion

Pressure-induced metallization and superconductivity in the layered van der Waals semiconductor GaTe

Jin Jiang,[1,2] Xuliang Chen (陈绪亮),[2,3,*] Shuyang Wang,[2,3] Chao An,[1] Ying Zhou,[1] Min Zhang,[1] Yonghui Zhou,[2,3] and Zhaorong Yang[1,2,3,†]

[1]*Institutes of Physical Science and Information Technology, Anhui University, Hefei 230601, China*
[2]*Anhui Province Key Laboratory of Condensed Matter Physics at Extreme Conditions, High Magnetic Field Laboratory, HFIPS, Chinese Academy of Sciences, Hefei 230031, China*
[3]*Collaborative Innovation Center of Advanced Microstructures, Nanjing 210093, China*

(Received 15 December 2022; revised 17 January 2023; accepted 19 January 2023; published 31 January 2023)

We present a systematic high-pressure study of layered van der Waals semiconductor GaTe through electrical transport, photoluminescence, and Raman spectroscopy measurements. We report observation of pressure-induced metallization and superconductivity (SC) in GaTe simultaneously occurring at ∼3 GPa, with an onset superconducting critical temperature of $T_C^{onset} \sim 5.0$ K. Analysis shows that a quasi–two-dimensional to three-dimensional structural crossover plays a crucial role in driving the observed metallization and SC. Upon further compression, T_C^{onset} first decreases gradually and then begins to increase above ∼10 GPa, displaying a V-shaped feature (SC-I→SC-II) due to a structural transition ($C2/m \rightarrow Fm$-$3m$). After reaching a local maximum of 4.5 K at ∼18 GPa, T_C^{onset} remains almost unchanged up to a highest pressure of 48.1 GPa. A comparison of the upper critical fields at different pressures spanning the SC-I and SC-II phases reveals that their pairing mechanisms may be different from each other. These results demonstrate that the band gap of layered semiconductor GaTe is highly tunable, which may stimulate further investigations by strain engineering, intercalation, and electrostatic doping.

DOI: 10.1103/PhysRevB.107.024512

I. INTRODUCTION

Band engineering in layered III–VI metal chalcogenides MXs (M = Ga, In; X = S, Se, Te) is an effective strategy to tailor their properties and explore emerging phenomena. In particular, GaTe has attracted much attention recently due to its remarkable properties and great application potentials [1–9]. At ambient conditions, GaTe crystallizes in a layered monoclinic structure [$C2/m$ space group; see Fig. 1(a)]. The intralayer bonds are mainly covalent and the interlayer bonds are of weak van der Waals type. Such a structural character of van der Waals interlayer interaction endows GaTe with layer-dependent band structures and properties. For bulk GaTe, it is a p-type semiconductor and has a direct band gap of 1.65 eV at room temperature, which is of vital importance in potential applications like solar cells and radiation detectors [8,9]. When thinning down from bulk to some critical number of layers, its band gap can exhibit a unique direct-indirect transition [1]. Such a process in GaTe and related layered semiconductors [10–13] creates Mexican-hat-shaped dispersion of the top valence band, resulting in a large density of states near the band edge and signaling a Van Hove singularity which may lead to magnetic and superconducting instabilities under external tuning parameters. In addition, the number of GaTe layers has profound influence on the in-plane anisotropic electronic structure [2,3], which is manifested as in-plane optical anisotropy in layered GaTe [2] as well as a high on/off ratio of 10^7 and retention time of 10^5 s in few-layered GaTe floating gate memory [3]. The transistor fabricated from multilayer GaTe exhibits a high photoresponsivity of 10^4 A/W and a very fast response speed of 6 ms [4], which promises it a candidate for future optoelectronic and photosensitive device applications. Interestingly, exposing GaTe to air can alter its band gap effectively from 1.65 to below 0.8 eV, and a significant conduction-band restructuring occurs via oxygen chemisorbed to the Te-terminated surfaces [5].

Inspired by the above results, it thus is natural and highly desirable to tune physical properties of GaTe via changing the lattice and layer coupling by the application of external pressure. Yet, to date, its high-pressure properties have not been well understood due to the lack of sufficient experimental data. A previous investigation on high-pressure Raman spectroscopy of GaTe found a monotonic increment of all Raman-active vibrational modes but the highest pressure investigated is only limited to 1.1 GPa [14]. Both x-ray diffraction (XRD) [15] and x-ray absorption spectroscopy [16] experiments show that GaTe undergoes a structural phase transition from the pristine monoclinic to a high-pressure cubic structure (Fm-$3m$ space group) at ∼10 GPa. In addition, a pressure-driven semiconductor-to-metal transition was inferred from optical reflectivity spectra measurements [15], which was thought to be accompanied with the structural transition. While the room-temperature

*xlchen@hmfl.ac.cn
†zryang@issp.ac.cn

 ©2023 American Physical Society

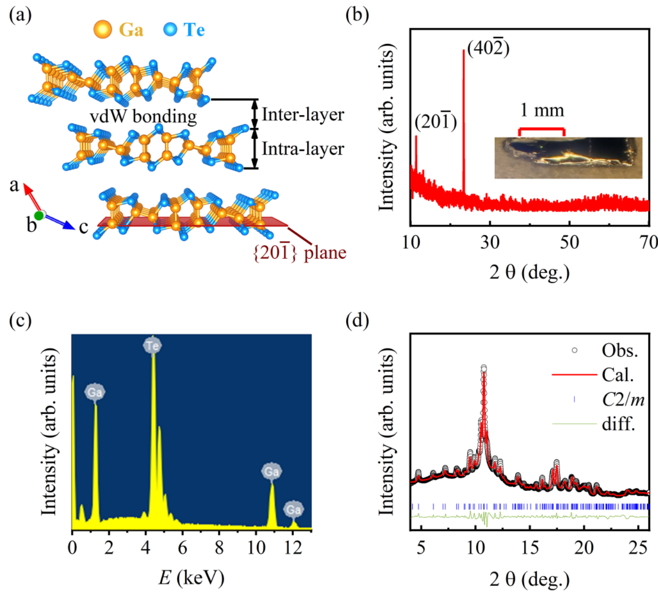

FIG. 1. (a) Schematic of the GaTe lattice structure. The Ga and Te atoms are represented by golden and blue spheres, respectively. (b) Single-crystal XRD pattern of GaTe. The inset shows a photo of a piece of as-grown GaTe single crystal. (c) Energy-dispersive x-ray spectroscopy of GaTe. (d) Powder XRD pattern. Red solid line is standard Rietveld refinement to the data (black circle).

resistivity, thermal conductivity, and Seebeck coefficient for GaTe were investigated with pressure to ∼10 GPa and it appears to trend towards metallic behavior [17], there is a distinct lack of definitive information regarding its metallization upon compression.

In this paper, electrical transport, Raman scattering, and photoluminescence (PL) spectroscopy measurements have been performed on the layered van der Waals semiconductor GaTe at pressures up to 48.1 GPa in diamond-anvil cells. We find that GaTe becomes metallic at ∼3 GPa, consistently observed from the electrical conductivity and PL data; simultaneously, superconductivity (SC) is observed with an onset critical temperature of $T_C^{\text{onset}}s \sim 5.0\,\text{K}$. Analysis indicates that the metallization and SC in GaTe may be tuned due to a pressure-induced dimensional crossover. The Raman data, in addition to previous XRD measurements, evidence a structural transition at ∼10 GPa, and correspondingly the evolution of T_C^{onset} displays a V-shaped feature relating to a SC-I→SC-II transition. Finally, the upper critical fields measured at various pressures imply that the two superconducting phases have different pairing mechanisms.

II. METHODS

GaTe single crystals were synthesized by a solid-state melting method. High-purity tellurium (99.99%, Alfa Aesar) and gallium (99.999%, Alfa Aesar) with the atomic ratio of 1:1 were mixed and loaded into an evacuated quartz tube. The tube was heated to 870 °C at 2 °C/min and kept for an hour, then quickly reduced to 850 °C for a week. Crystals of GaTe with black surface were obtained, as displayed in the inset of Fig. 1(b). The single-crystal XRD pattern was collected by using an in-lab x-ray diffractometer (Cu Kα, $\lambda = 1.5406$ Å). Powder XRD was measured at the beamline BL15U1 of the Shanghai Synchrotron Radiation Facility ($\lambda = 0.6199$ Å). The atomic ratio was characterized by the energy-dispersive x-ray spectra (EDXS). Ambient-pressure photoluminescence (PL, 633-nm laser) and Raman- (532-nm laser) scattering measurements were performed with a Renishaw inVia microscope system at a high-vacuum environment ($\sim 10^{-5}$ Pa) [18]. The laser beam was focused on the sample by a 20× objective and the laser power was kept below 0.5 mW in order to reduce the laser heating effect and protect the sample from damage.

High-pressure Raman scattering and PL emission experiments were carried out by using symmetric diamond-anvil cells (DACs), with T301 stainless steel as the gasket and NaCl as the pressure-transmitting medium. A piece of freshly exfoliated single crystal of GaTe was loaded. A standard four-probe method was used for high-pressure electrical transport measurements by using Pt foil as the electric lead, by using a nonmagnetic Be-Cu alloy diamond-anvil cell. The culet of the diamond anvils is 300 μm and the pressure is calibrated at room temperature by using the ruby fluorescence method.

III. RESULTS AND DISCUSSION

Bulk GaTe is a layered material with a monoclinic ($C2/m$ space group) structure. The schematic crystal structure of GaTe is shown in Fig. 1(a). The intralayer atoms consist of alternating Te-Ga-Ga-Te layers, predominantly covalently bonded. The layers are stacked to each other perpendicular to the {20-1} family of planes by van der Waals forces. Single-crystal and powder XRD patterns of the samples are shown in Figs. 1(b) and 1(d). The single-crystal XRD data reveal that the {20-1} family of planes is the natural cleavage facet of as-grown GaTe single crystals. Powder XRD was analyzed by the standard Rietveld refinement method. The extracted lattice parameters from the fit are $a = 17.45(5)$ Å, $b = 4.08(2)$ Å, $c = 17.95(7)$ Å, and $\beta = 145.64(4)$, in agreement with the previous report [19]. The EDXS measurements give the atomic ratio of Ga:Te as 1.01:0.99 [Fig. 1(c)]. All these characterizations demonstrate high quality of our samples studied.

Figure 2 plots the temperature (1.8–300 K) dependence of the resistance R of GaTe at various pressures up to 48.1 GPa. Starting at 1.0 GPa, GaTe shows a semiconducting conduction behavior ($dR/dT < 0$) as it is at ambient pressure [20]. At 3.3 GPa, however, the resistance decreases significantly upon cooling [$dR/dT > 0$; see Fig. 2(b)], exhibiting more than 5 orders of magnitude reduction in resistance. This observation indicates partial metallization of GaTe in a percolation manner. Strikingly, accompanied with this semiconductor-to-metal transition, a low-temperature drop in resistance starts to occur at an onset temperature of $T_C^{\text{onset}} \sim 5.0\,\text{K}$ and zero resistance is observed at ∼3.0 K [Fig. 2(d)], indicating pressure-induced SC in GaTe. T_C^{onset} decreases with increasing pressure and reaches a minimum of 2.9 K at 7.8 GPa. Further increasing the pressure from 10.3 to 18.1 GPa leads to a gradual increment of T_C^{onset} [Fig. 2(e)]. Meanwhile, T_C^{onset} reaches a local maximum of 4.6 K and zero resistance is observed once again above 15.0 GPa. Above 18.1 GPa, the superconducting transition becomes very sharp and T_C^{onset} re-

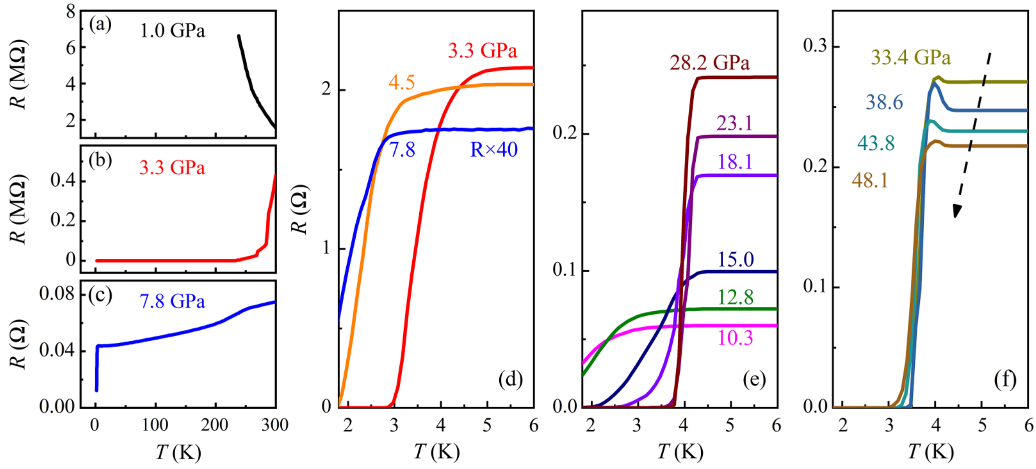

FIG. 2. (a)–(c) Temperature-dependent in-plane resistance in the temperature range of 1.8–300 K. Resistance of the low-temperature region in pressure range of 3.3 to 7.8 GPa (d), 10.3 to 28.2 GPa (e), and 33.4 to 48.1 GPa (f).

mains almost unchanged with pressure. Note that there is a tiny upturn in low-temperature resistance at and above 33.4 GPa, which may indicate a fragile precursor for SC as observed in pressurized MoP [21].

Next, we measured the $R(T)$ curves under applied magnetic fields perpendicular to the layer of the sample. As shown in Fig. 3, we performed these measurements by choosing three different pressure points of 3.3, 18.0, and 33.4 GPa locating below and above the critical pressure of ∼10 GPa around which a T_C^{onset} minimum is observed. As expected, the resistance drop gets suppressed gradually with increasing field, further confirming the presence of SC in GaTe under pressure. Here, the upper critical field $\mu_0 H_{C2}(T)$ is defined from the resistance criterion $R_{\text{cri}} = 90\% R_{\text{n}}$ (R_{n} represents the normal-state resistance). The temperature–magnetic-field phase diagrams are constructed in Figs. 3(d)–3(f). The empirical Ginzburg–Landau (GL) equation [22] is used to estimate the zero-temperature values of $\mu_0 H_{C2}(0)$, which yields 9.75 T at 3.3 GPa, 2.03 T at 18.0 GPa, and 2.02 T at 33.4 GPa. The relatively high upper critical field indicates that the observed superconductivity may be of bulk in nature, in spite of no magnetic susceptibility data.

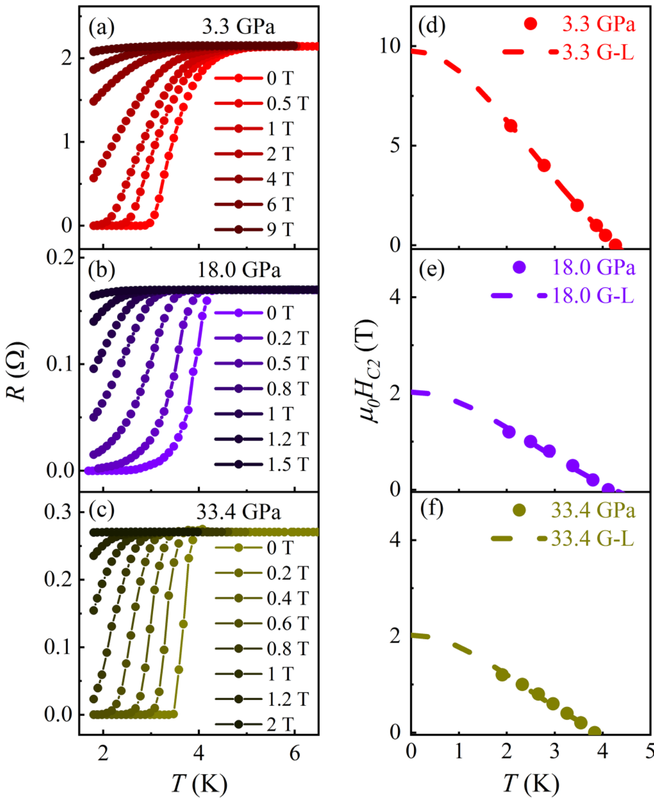

FIG. 3. (a)–(c) Temperature dependence of resistance under different magnetic fields perpendicular to the layer plane at 3.3,18, and 33.4 GPa, respectively. (d)–(f) Upper critical field $\mu_0 H_{C2}$ vs Tc at various pressures. Dashed lines represent the fits to the empirical Ginzburg-Landau (GL) formula.

In order to trace the evolution of the band gap of GaTe under pressure, we performed PL measurements at room temperature. At ambient pressure, a single narrow PL peak centered at 750 nm was observed [Fig. 4(a)], in line with previous reports [2,3,5–7]. This corresponds to a peak energy of ∼1.65 eV, which is exactly the size of the intrinsic direct band gap of GaTe at the Z point [2,23,24]. Figure 4(b) exhibits the PL spectra at several pressures. One can see that the PL intensity gets suppressed rapidly and the PL intensity is almost vanishing above 3.1 GPa. Since this critical pressure is similar to that from the above transport experiment, the vanishing of PL intensity should be related to the pressure-induced metallization. At the same time, the position of the PL peak increases with pressure. This corresponds to a linear decrease in PL peak energy from 1.65 eV at ambient pressure to 1.48 eV at 3.1 GPa, as shown in Fig. 4(c).

In order to investigate whether or not the above observed anomalies relate to changes of the structure, Raman spectra under pressure were collected. As displayed in Fig. 5(a), the Raman spectrum at ambient pressure exhibits 12 modes marked as A_g^1 to A_g^{10} and B_g^1 to B_g^2, in good agreement with the previous results [2,3]. Figure 5(b) displays the Raman spectra of GaTe at various pressures to 20.1 GPa. In general, all the Raman modes show a blueshift in frequency under pressure, owing to shrinkage of the lattice and the increment in interactions which results in the enhancement of the

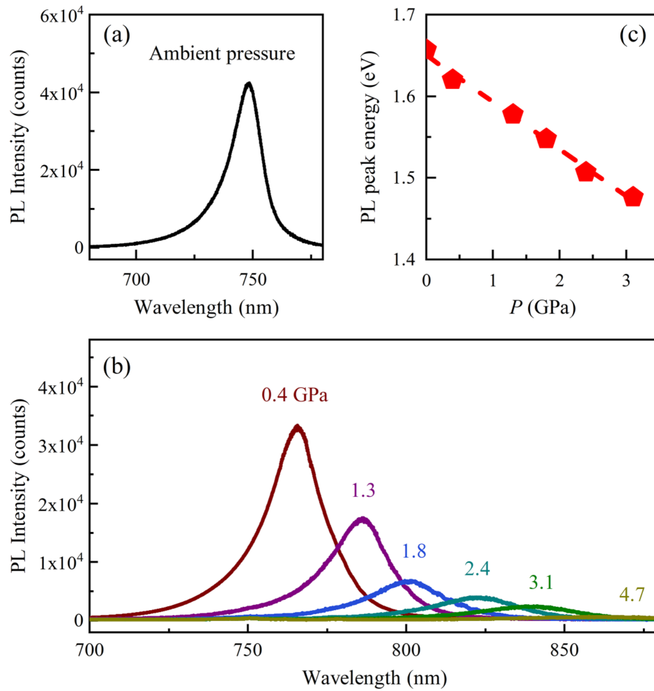

FIG. 4. (a) PL spectrum of GaTe at ambient pressure. (b) PL spectra at high pressures from 0.4 to 4.7 GPa. (c) Pressure dependence of the PL peak energy. The dashed line is a least-square fit to the experimental points.

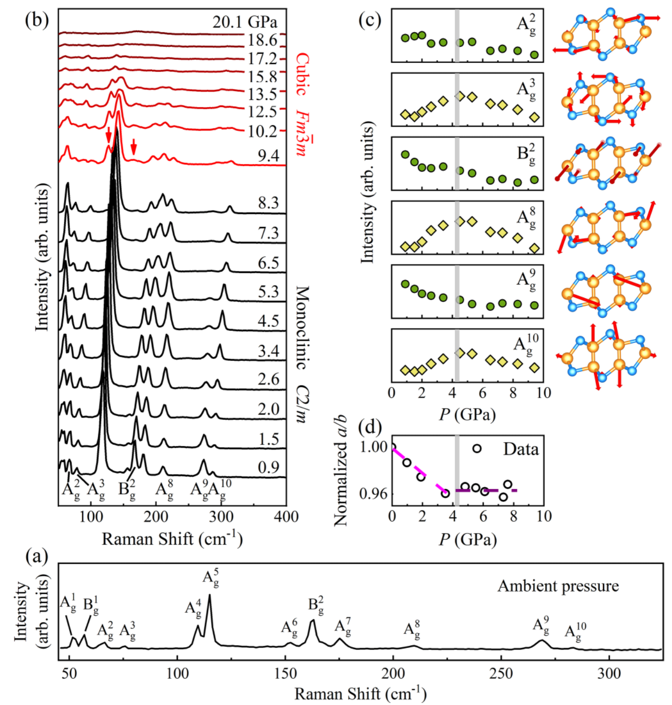

FIG. 5. (a) Raman spectrum of GaTe at ambient pressure. (b) Pressure dependence of Raman spectra at various pressures. (c) Intensity evolution of several separate modes as a function of pressure (left column). Corresponding atomic vibrational motions for each separate mode from Ref. [2]. (d) Normalized cell parameters ratio a/b for the monoclinic GaTe at various pressures to 7.8 GPa calculated based on XRD data in Ref. [15].

effective restoring forces acting on the atoms. Clearly, when the pressure increases beyond 9.4 GPa, the Raman modes from the pristine structural phase of GaTe weaken suddenly and some new modes emerge, as indicated by arrows. These observations can be ascribed to a monoclinic ($C2/m$) to cubic (Fm-$3m$) structural phase transition [15].

If examining the Raman data more carefully, one can see an additional feature around 4 GPa, i.e., the intensity evolution of some Raman modes is nonmonotonic. We selected some separate peaks to plot their intensity versus pressure relations in Fig. 5(c). Obviously, the intensity of the A_g^3, A_g^8, and A_g^{10} modes shows a maximum around 4 GPa, while that of the A_g^2, B_g^2, and A_g^9 modes decreases monotonically. We plot together the corresponding vibration patterns for each Raman mode [2]. It is noticed that for the A_g^3, A_g^8, and A_g^{10} modes the projection of vibrational vector is mainly along the out-of-plane direction and for the A_g^2, B_g^2, and A_g^9 modes it is mainly or solely along the in-plane direction. Recall that the lattice of GaTe is built up of stacking Te-Ga-Ga-Te layers held together by weak van der Waals interactions [Fig. 1(a)]. Combining all these factors led us to propose that pressure-induced anomalous strengthening of the interlayer coupling should play a significant role in driving the nonmonotonic evolution of the mode intensity and the metallization and SC. This conclusion is further substantiated by the pressure-dependent normalized lattice ratio a/b calculated based on the XRD data in Ref. [15]. As exhibited in Fig. 5(d), it first decreases rapidly due to weak interlay coupling of van der Waals type and thereby larger interlayer compression rate. With the interlayer coupling being strong enough, the normalized lattice ratio a/b then maintains constant with pressure, resembling a three-dimensional atomic network bonded by strong Coulomb interaction. In fact, such a role of strong Coulomb interaction between layers in affecting the Raman intensity has been revealed in its sister layered van der Waals semiconductors InSe and GaSe [13,25], in spite of some difference in lattice between them at ambient pressure.

We summarize the main results in the phase diagram of Fig. 6. As discussed above, a crossover of the bonding type between layers of GaTe occurs, presumably from the weak van der Waals to strong Coulomb interaction. The formation of strong Coulomb interaction between layers tunes GaTe from quasi–two-dimensional (quasi-2D) to three dimensional (3D), which modifies its band structure dramatically and results in the pressure-induced metallization and SC at ∼3–4 GPa. Indeed, there have been several reports on a pressure-induced quasi-2D to 3D structural crossover in layered systems [26–29], where a similar behavior of the lattice ratio is observed, i.e., it first decreases and then almost flattens above a critical pressure [Fig. 5(d)]. In addition, pressure-induced metallization and/or anomalous evolution in Raman mode intensity in some semiconducting systems are also observed [26,28]. On the other hand, a sizable band gap of 1.48 eV at 3.1 GPa observed from the PL [Fig. 4(c)] suggests that the metallization is not from closure of its direct band gap at the Z point but probably due to formation of an indirect band gap at some other momentum point and a Mexican-hat-shaped valence band that crosses over the Fermi level, i.e., an electronic topological transition (electronic structure change not associated with a crystal structure change) [17]. This process may be in analogy to that observed in 2D III–VI

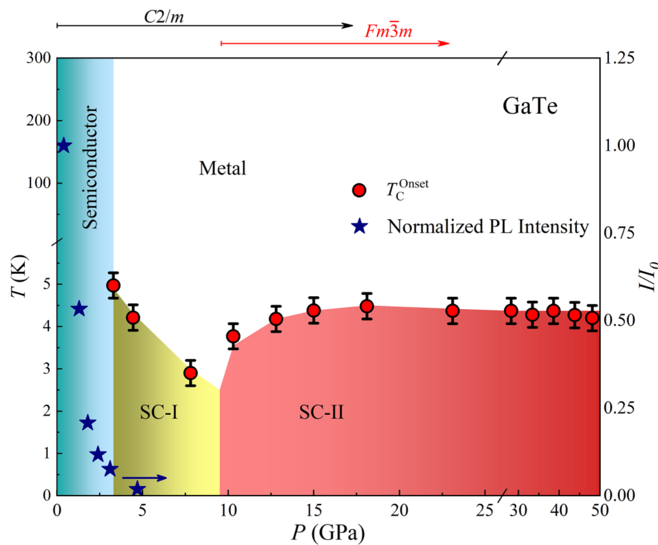

FIG. 6. Temperature-pressure phase diagram of GaTe. SC-I and SC-II stand for the two superconducting phases of GaTe under pressure due to a structural transition.

*MX*s [11], where the Mexican-hat-shaped valence band especially predisposes them for the potential phenomena under external stimuli like unconventional superconductivity. Obviously, further studies especially from high-pressure theoretical calculations may be favorable to clarify this issue.

Furthermore, T_C^{onset} shows a V-shaped feature due to a pressure-induced structural transition. After completion of the structural transition above ~18 GPa [Fig. 5(b)], T_C^{onset} stops to increase and exhibits a saturating behavior. It is known that the upper critical field $\mu_0 H_{C2}(T)$ is closely related to the pairing mechanism of SC. From Fig. 3, we have obtained the $\mu_0 H_{C2}(0)$ at zero temperature, i.e., 9.75 T at 3.3 GPa, 2.03 T at 18.0 GPa, and 2.02 T at 33.4 GPa. As the T_C^{onset} is nearly equal, the weak-coupling Pauli paramagnetic limit [30] of $\mu_0 H_P(0) = 1.84 T_C = 7.86\,\text{T}$ at zero temperature is thus almost the same for these three pressure points. Consequently, $\mu_0 H_{C2}(0)$ is larger than $\mu_0 H_P(0)$ at 3.3 GPa, while $\mu_0 H_{C2}(0)$ is much smaller than $\mu_0 H_P(0)$ at 18.0 and 33.4 GPa. This means that the pairing mechanisms should be different for the SC-I and SC-II phases.

IV. CONCLUSIONS

In summary, by using external pressure as a tuning knob, we have investigated the electrical transport, Raman spectroscopy, and PL properties of layered van der Waals semiconductor GaTe. We found that this material shows a semiconductor-to-metal transition and SC simultaneously occurring at ~3 GPa. These are related to a quasi-2D to 3D crossover due to change of the bonding nature between layers from the weak van der Waals type to the strong Coulomb type. T_C^{onset} displays a V-shaped feature in the pressure range of 3.3–18 GPa, signaling a SC-I to SC-II transition due to a monoclinic to cubic structural transition followed by a nearly constant evolution behavior against pressure up to 48.1 GPa. Analysis of the upper critical fields suggests that the SC-I and SC-II phases have different pairing mechanisms. The relatively small critical pressure of ~3 GPa indicates that the band gap of GaTe is highly tunable, which may stimulate further investigations on this material by intercalation and electrostatic doping. As a comparison, a similar situation is also encountered in the well-known layered van der Waals semiconductor MoS_2 [31–35], where metallization and SC occur at high pressures of ~60 and ~90 GPa, respectively.

ACKNOWLEDGMENTS

This work was financially supported by the National Key R&D Program of China (Grants No. 2022YFA1602603 and No. 2018YFA0305704), the National Natural Science Foundation of China (Grants No. 12174395, No. U19A2093, No. 12004004, and No. 12204004), the Users with Excellence Program of Hefei Center CAS (Grant No. 2021HSC-UE008), and the Key Project of Natural Scientific Research of Universities in Anhui Province (Grants No. KJ2021A0068 and No. KJ2021A0064). Yonghui Zhou was supported by the Youth Innovation Promotion Association CAS (Grant No. 2020443).

[1] K. Lai, S. Ju, H. Zhu, H. Wang, H. Wu, B. Yang, E. Zhang, M. Yang, F. Li, S. Cui, X. Deng, Z. Han, M. Zhu, and J. Dai, Strong bulk-surface interaction dominated in-plane anisotropy of electronic structure in GaTe, Commun. Phys. **5**, 143 (2022).

[2] S. Huang, Y. Tatsumi, X. Ling, H. Guo, Z. Wang, G. Watson, A. A. Puretzky, D. B. Geohegan, J. Kong, J. Li, T. Yang, R. Saito, and M. S. Dresselhaus, In-plane optical anisotropy of layered Gallium telluride, ACS Nano **10**, 8964 (2016).

[3] H. Wang, M.-L. Chen, M. Zhu, Y. Wang, B. Dong, X. Sun, X. Zhang, S. Cao, X. Li, J. Huang, L. Zhang, W. Liu, D. Sun, Y. Ye, K. Song, J. Wang, Y. Han, T. Yang, H. Guo, C. Qin, L. Xiao, J. Zhang, J. Chen, Z. Han, and Z. Zhang, Gate tunable giant anisotropic resistance in ultra-thin GaTe, Nat. Commun. **10**, 2302 (2019).

[4] F. Liu, H. Shimotani, H. Shang, T. Kanagasekaran, V. Zólyomi, N. Drummond, V. I. Fal'ko, and K. Tanigaki, High-sensitivity photodetectors based on multilayer GaTe flakes, ACS Nano **8**, 752 (2014).

[5] J. J. Fonseca, S. Tongay, M. Topsakal, A. R. Chew, A. J. Lin, C. Ko, A. V. Luce, A. Salleo, J. Wu, and O. D. Dubon, Bandgap restructuring of the layered semiconductor gallium telluride in air, Adv. Mater. **28**, 6465 (2016).

[6] P. Hu, J. Zhang, M. Yoon, X.-F. Qiao, X. Zhang, W. Feng, P. Tan, W. Zheng, J. Liu, X. Wang, J. C. Idrobo, D. B. Geohegan, and K. Xiao, Highly sensitive phototransistors based on two-dimensional GaTe nanosheets with direct bandgap, Nano Res. **7**, 694 (2014).

[7] H. Cai, B. Chen, G. Wang, E. Soignard, A. Khosravi, M. Manca, X. Marie, S. L. Y. Chang, B. Urbaszek, and S. Tongay, Synthesis of highly anisotropic semiconducting GaTe nanomaterials and emerging properties enabled by epitaxy, Adv. Mater. **29**, 1605551 (2017).

[8] K. C. Mandal, S. Das, R. Krishna, P. G. Muzykov, S. Ma, and F. Zhao, Surface passivation of p-GaTe layered crystals for improved p-GaTe/n-InSe heterojunction solar cells, Mater. Res. Soc. Symp. Proc. **1268**, 210 (2011).

[9] K. C. Mandal, R. M. Krishna, T. C. Hayes, P. G. Muzykov, S. Das, T. S. Sudarshan, and S. Ma, Layered GaTe crystals for radiation detectors, IEEE Trans. Nucl. Sci. **58**, 1981 (2011).

[10] T. Cao, Z. Li, and S. G. Louie, Tunable Magnetism and Half-Metallicity in Hole-Doped Monolayer GaSe, Phys. Rev. Lett. **114**, 236602 (2015).

[11] H. Cai, Y. Gu, Y.-C. Lin, Y. Yu, D. B. Geohegan, and K. Xiao, Synthesis and emerging properties of 2D layered III–VI metal chalcogenides, Appl. Phys. Rev. **6**, 041312 (2019).

[12] D. Barragan-Yani, J. M. Polfus, and L. Wirtz, Native defects in monolayer GaS and GaSe: Electrical properties and thermodynamic stability, Phys. Rev. Mater. **6**, 114002 (2022).

[13] M. Bejani, O. Pulci, N. Karimi, E. Cannuccia, and F. Bechstedt, Electronic structure, vibrational properties, and optical spectra of two- and three-dimensional hexagonal InSe: Layer-dependent ab initio calculations, Phys. Rev. Mater. **6**, 115201 (2022).

[14] K. R. Allahverdiev, S. S. Babaev, E. Y. Salaev, M. M. Tagyev, E. A. Vinogradov, A. F. Goncharov, N. N. Melnick, S. I. Subbotin, and V. V. Panfilov, Raman scattering in GaTe under hydrostatic pressure, Solid State Commun. **35**, 705 (1980).

[15] U. Schwarz, K. Syassen, and R. Kniep, Structural phase transition of GaTe at high pressure, J. Alloys Compd. **224**, 212 (1995).

[16] J. Pellicer-Porres, A. Segura, V. Muñoz, and A. San Miguel, High-pressure x-ray absorption study of GaTe including polarization, Phys. Rev. B **61**, 125 (2000).

[17] M. K. Jacobsen, Y. Meng, R. S. Kumar, and A. L. Cornelius, High pressure structural and transport measurements of InTe, GaTe, and $InGaTe_2$, J. Phys. Chem. Solids **74**, 723 (2013).

[18] S. Wang, X. Chen, C. An, Y. Zhou, M. Zhang, Y. Zhou, Y. Han, and Z. Yang, Observation of room-temperature amplitude mode in quasi-one-dimensional charge-density-wave material CuTe, Appl. Phys. Lett. **120**, 151902 (2022).

[19] M. Julien-Pouzol, S. Jaulmes, M. Guittard, and F. Alapini, Monotellurure de gallium, GaTe, Acta Crystallogr., Sect. B **35**, 2848 (1979).

[20] D. N. Bose and S. Pal, Photoconductivity, low-temperature conductivity, and magnetoresistance studies on the layered semiconductor GaTe, Phys. Rev. B **63**, 235321 (2001).

[21] Z. Chi, X. Chen, C. An, L. Yang, J. Zhao, Z. Feng, Y. Zhou, Y. Zhou, C. Gu, B. Zhang, Y. Yuan, C. Kenney-Benson, W. Yang, G. Wu, X. Wan, Y. Shi, X. Yang, and Z. Yang, Pressure-induced superconductivity in MoP, npj Quantum Mater. **3**, 28 (2018).

[22] M. Tinkham, Effect of fluxoid quantization on transitions of superconducting films, Phys. Rev. **129**, 2413 (1963).

[23] J. F. Sánchez-Royo, J. Pellicer-Porres, A. Segura, V. Muñoz-Sanjosé, G. Tobías, P. Ordejón, E. Canadell, and Y. Huttel, Angle-resolved photoemission study and first-principles calculation of the electronic structure of GaTe, Phys. Rev. B **65**, 115201 (2002).

[24] A. Yamamoto, A. Syouji, T. Goto, E. Kulatov, K. Ohno, Y. Kawazoe, K. Uchida, and N. Miura, Excitons and band structure of highly anisotropic GaTe single crystals, Phys. Rev. B **64**, 035210 (2001).

[25] M. K. Niranjan, Significance of Coulomb interaction in interlayer coupling, polarized Raman intensities, and infrared activities in the layered van der Waals semiconductor GaSe, Phys. Rev. B **103**, 195437 (2021).

[26] Z. Zhao, H. Zhang, H. Yuan, S. Wang, Y. Lin, Q. Zeng, G. Xu, Z. Liu, G. K. Solanki, K. D. Patel, Y. Cui, H. Y. Hwang, and W. L. Mao, Pressure induced metallization with absence of structural transition in layered molybdenum diselenide, Nat. Commun. **6**, 7312 (2015).

[27] F. Yu, X. Zhu, X. Wen, Z. Gui, Z. Li, Y. Han, T. Wu, Z. Wang, Z. Xiang, Z. Qiao, J. Ying, and X. Chen, Pressure-Induced Dimensional Crossover in a Kagome Superconductor, Phys. Rev. Lett. **128**, 077001 (2022).

[28] V. Rajaji, U. Dutta, P. C. Sreeparvathy, S. C. Sarma, Y. A. Sorb, B. Joseph, S. Sahoo, S. C. Peter, V. Kanchana, and C. Narayana, Structural, vibrational, and electrical properties of 1T-$TiTe_2$ under hydrostatic pressure: Experiments and theory, Phys. Rev. B **97**, 085107 (2018).

[29] X. Ma, Y. Wang, Y. Yin, B. Yue, J. Dai, J. Cheng, J. Ji, F. Jin, F. Hong, J.-T. Wang, Q. Zhang, and X. Yu, Dimensional crossover tuned by pressure in layered magnetic $NiPS_3$, Sci. China Phys. Mech. Astron. **64**, 297011 (2021).

[30] A. M. Clogston, Upper Limit for the Critical Field in Hard Superconductors, Phys. Rev. Lett. **9**, 266 (1962).

[31] R. B. Somoano and A. Rembaum, Superconductivity in Intercalated Molybdenum Disulfide, Phys. Rev. Lett. **27**, 402 (1971).

[32] R. B. Somoano, V. Hadek, and A. Rembaum, Alkali metal intercalates of molybdenum disulfide, J. Chem. Phys. **58**, 697 (1973).

[33] Z.-H. Chi, X.-M. Zhao, H. Zhang, A. F. Goncharov, S. S. Lobanov, T. Kagayama, M. Sakata, and X.-J. Chen, Pressure-Induced Metallization of Molybdenum Disulfide, Phys. Rev. Lett. **113**, 036802 (2014).

[34] J. T. Ye, Y. J. Zhang, R. Akashi, M. S. Bahramy, R. Arita, and Y. Iwasa, Superconducting dome in a gate-tuned band insulator, Science **338**, 1193 (2012).

[35] Z. Chi, X. Chen, F. Yen, F. Peng, Y. Zhou, J. Zhu, Y. Zhang, X. Liu, C. Lin, S. Chu, Y. Li, J. Zhao, T. Kagayama, Y. Ma, and Z. Yang, Superconductivity in Pristine $2H_a$-MoS_2 at Ultrahigh Pressure, Phys. Rev. Lett. **120**, 037002 (2018).